International Journal of ChemTech Research
CODEN (USA): IJCRGG, ISSN: 0974-4290, ISSN(Online):2455-9555
Vol.9, No.08 pp 319-327, 2016

Ruthenium Bipyridine Dichloride Complex Sensitized Cadmium Doped TiO_2 and SnO_2 Nanocrystals

S. Chitra[1]*, D. Easwaramoorthy[2]

[1]Department of Chemistry, Jeppiaar Engineering College, Chennai, India
[2]Department of Chemistry, B.S.Abdur Rahman University, Chennai, India

Abstract : Many semiconductor oxide layers were coated over TiO_2 which acts as the photoanodic materials in Dye Sensitized Solar Cells (DSSCs). A suitable dye sensitizer coated over the suitable photoanodic material could be used in DSSC to increase the efficiency to a higher rate. This paper deals with the photoconductivity and electrical studies of the cadmium doped TiO_2 and SnO_2 nanocrystals coated with the $[Ru(bipy)_2(C_6H_5NHNH_2)]Cl_2$ as the dye sensitizer which could be used in DSSC in future.
Keywords : DSSC, Photoanode, Photoconductivity, Dye sensitizer.

1. Introduction

The rapidly increasing fossil fuel consumption and excessive greenhouse gas emissions have put significant pressure on exhaustive global energy demand. Photoelectrochemical cells have led to the development of efficient and low-cost dye sensitized solar cells (DSSCs) at the laboratory level. DSSCs have emerged as an attractive choice for solar energy harvesting since their invention[1-5]. Many efforts had been carried out to improve the cell performance by (a) increasing the cell conductivity, (b) minimizing the electron recombination at TiO_2-dye interface, (c) enhancing the regeneration kinetics at the cathode, (d) enhancing the photovoltage by changing the redox mediator electrolyte, (e) improving the light harvesting efficiency by using reflection/scattering layers, plasmonic materials, or new dyes. Recently, improving the conversion efficiency of DSSCs by doping one kind of metal ion in TiO_2 which act as the photoanode had been mostly investigated[6]. The role of cadmium ions in the DSSC is of particular interest. The incorporation of cadmium into the host TiO_2 and SnO_2 lattices increases the conductivity. Among the sensitizers which could be used in DSSCs, the Ruthenium complexes and organic dyes have the best photovoltaic performances both in terms of conversion yield and long term stability[7-16].

In the present study, 5 mole % Cd^{2+} doped TiO_2 (CTO) and 5 mole % Cd^{2+} doped SnO_2 (CSO) were identified as the better semiconductor oxide layer and was coated with phenyl hydrazine substituted Ruthenium $(Bi\text{-}pyridine)_3]Cl_2$ complex (PHRBP) which could be used in DSSCs in future.

2. Materials and Methods:

Cadmium doped TiO_2 and SnO_2 (CTO and CSO) nanocrystals was synthesized by microwave solvothermal method[17,18] and phenyl hydrazine substituted Ruthenium $(Bi\text{-}pyridine)_3]Cl_2$ complex (PHRBP) was synthesized by refluxing method[19]. Also, in the present study, $[Ru(bipy)_2(C_6H_5NHNH_2)]Cl_2$ complex was coated as the dye sensitizer over the Cadmium doped TiO_2 and SnO_2 (CTO and CSO) nanocrystals compacted as disc shaped pellet. In the present study dark & photo current were recorded for $[Ru(bipy)_2(C_6H_5NHNH_2)]Cl_2$

as the dye sensitizer coated over the cadmium doped TiO_2 and SnO_2 nanocrystals and the time-resolved rise and decay of photocurrent spectra was also recorded.

DC electrical conductivity measurements were carried out to an accuracy of ± 1% for all the synthesized nanocrystals and photosensitizer materials using the conventional two-probe technique in a way similar to that followed by Mahadevan and his co-workers[20-22]. The measurements were made at various temperatures ranging from 30-150 ºC. The capacitance (C) and dielectric loss factor (tanδ) measurements were carried out to an accuracy of ± 1 % with Agilant 4284A LCR meter in the temperature range of 30 - 150°C and with fixed 1 kHz frequency.

3. Results and Discussions

3.1 Photoconductivity Studies

The variation of field dependence dark current (I_d) and photocurrent (I_p) with applied voltage (V) for PHTCO and PHCSO samples were shown in Figures 3.1.1 - 3.1.2. It was observed that both dark and photo currents of dye sensitized cadmium doped TiO_2 and SnO_2 nanocrystals increased linearly with the applied voltage. The photocurrent of both PHTCO and PHCSO nanocrystals was more than the dark current, which was termed as positive photoconductivity.

The variation of dark and photocurrent for PHCTO and PHCSO nanocrystals in Ln - Ln scale were shown in Figures 3.1.3 - 3.1.4. From the plots, Ln (I_d) *vs* Ln(V) and Ln (I_p) *vs* Ln (V) were found to be linear ($r \approx 1$) and super-linear ($r > 1$) respectively. Super-linear behavior suggested that extra carriers were generated and entered into the conduction band of the samples. The variation of dark and photocurrent for desensitized (CTO and CSO) and PHRBP complex sensitized CTO and CSO (PHCTO and PHCSO) samples were shown in Figures 3.1.5 - 3.1.6.

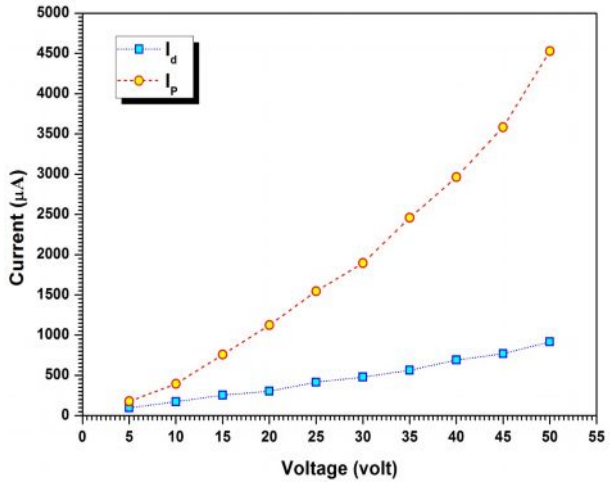

Fig 3.1.1

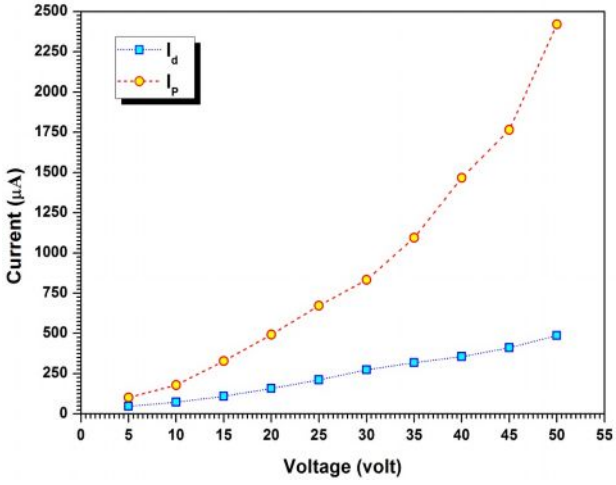

Fig 3.1.2

Figure 3.1.1 & 3.1.2Variation of dark and photo current with applied voltage for PHCTO & PHCSO nanocrystals

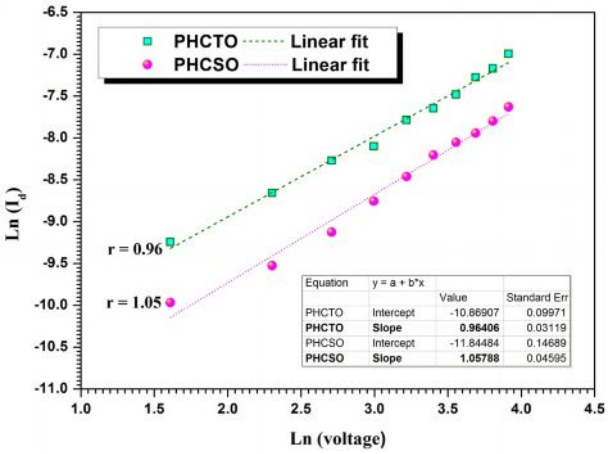

Fig 3.1.3

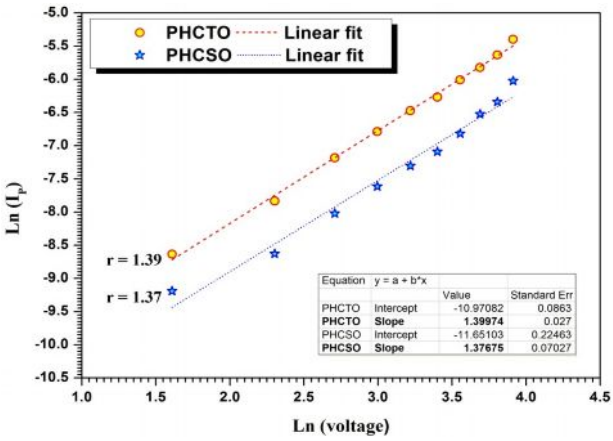

Fig 3.1.4

Fig 3.1.3 &3.1.4 Variation of Ln (I_d) *vs* Ln (V) & Ln (I_p) *vs* Ln (V)of PHCTO and PHCSO nanocrystals

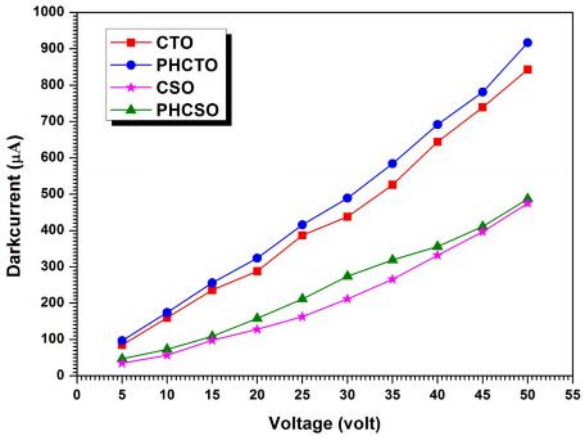

Fig 3.1.5

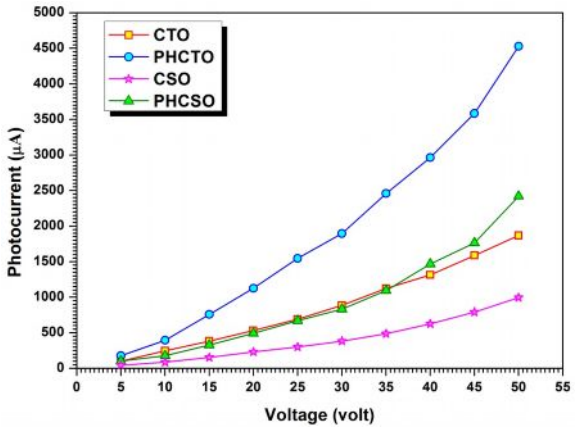

Fig 3.1.6

Fig 3.1.5 & 3.1.6 Variation of dark current & Photocurrent with applied voltage for desensitized and PHRBP complex sensitized CTO and CSO nanocrystals

More interestingly the photo current of PHRBP complex sensitized CTO and CSO (PHTCO and PHCSO) nanocrystals was highly enhanced (at 30 V field voltage) when compared to CTO and CSO samples by more than 2 orders. This might be due to the coated dye (PHRBP complex) could be attributed to higher electron injection yield to the nanocrystalline samples. Hence the PHRBP complexes could act as the sensitizer and transferred the excited electrons to the conduction band of CTO and CSO. The dark current for the sensitized samples were also slightly increased when compared to CTO and CSO samples.

In order to investigate the effect of intensity of illumination on the PHRBP complexes sensitized CTO and CSO samples, the samples were subjected to illuminate low intensity (75 watt, 288 lumens intensity) and high intensity light radiation (150 watt, 5600 lumens intensity). The recorded time-resolved rise and decay of photocurrent spectra for PHCTO and PHCSO samples was shown in Figure 3.1.7. It revealed that, under steady state illumination, the photocurrent for PHCTO sample increased rapidly and attained maximum value within short interval of time (~ 340 s). This was due to fast process of generation of electron–hole pairs as a result of absorption of photons. The maximum photocurrent generation in the sample was higher than that of desensitized sample (CTO).

After attaining maximum value of photocurrent it started decaying even during steady illumination irrespective with the intensity of illumination. This might be due to a few of the electron-hole pairs attracted by the imperfection centers present in the forbidden energy gap to attain saturation and produced steady

photocurrent. The PHRBP coated CTO and CSO samples attained the steady state much faster than that of desensitized sample (CTO and CSO). When illumination was switched off irrespective with the intensity of illumination the generation of electrons recombined with holes and was captured by re-adsorbed oxygen molecules. Hence the current decreased suddenly and attained constant value within few hundred seconds (~ 300 Sec Figure 6.7b).

However, as the intensity of the light increased from 75 W to 150 W, the electron recombined with holes and re-adsorbed oxygen molecules took slightly higher time than that of low intensity illumination. Recently, mesoporous TiO_2 nanoparticles showed a drastically enhanced photoelectrochemical response under visible light irradiation after entrapping a photosensitizer molecule (dye) inside the mesopores.

In the present study, the dye sensitized samples (PHCTO, PHCSO) produced enhanced dark and photocurrents roughly 3 times higher than that of dye sensitized mesoporous TiO_2 nanoparticles[23]. The efficient synthesis strategy and enhanced photoresponse of these pure and doped TiO_2 and SnO_2 semiconducting nanoparticles could make easier to design other semiconductor oxides as photoanodes and their applications in photon-to-electron conversion processes.

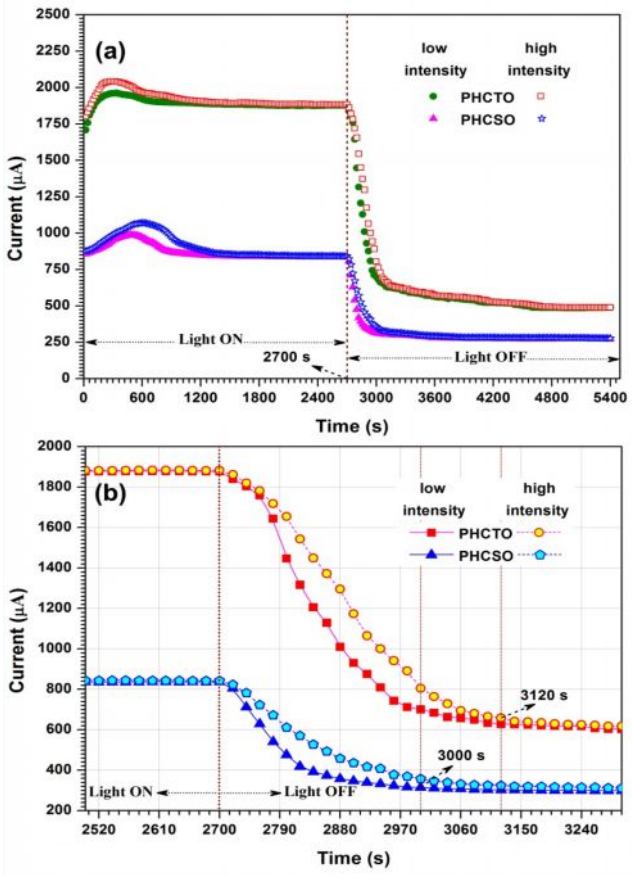

Fig 3.1.7

Fig 3.1.7 (a) Variation of time resolved rise and decay of photocurrent with different light intensity spectra of PHCTO and PHCSO nanocrystals (b) the same spectra in expanded scale

3.2 Electrical Properties

The variation of DC conductivity (σ_{dc}) of desensitized and PHRBP complexes sensitized CTO and CSO (PHCTO and PHCSO) nanocrystals with temperature was shown in Figure 3.2.1. From this figure, it could be seen that σ_{dc} increased with increase in temperature, indicating the semiconducting nature of the samples within the studied range of temperature (30 ºC to 150 ºC). The σ_{dc} for PHCTO and PHCSO samples were higher than by 2 orders when compared to CTO and CSO samples, respectively at room temperature (30ºC). This variation was almost same with all studied range of temperatures. The plot of 1000/T *vs* Ln σ_{dc} for PHCTO and PHCSO

nanocrystals for different temperatures was shown in Figure 3.2.2. The activation energies (ΔE_{dc}) were calculated from the slope of the straight line best fitted by least square analysis and the pre-exponential factor (σ_o) was calculated by the intercept of the straight line on Y-axis. The calculated activation energy and pre-exponential factor values were given in Table 3.2.1.

At low temperatures, most of the free carriers in a semiconductor did not have sufficient energy to jump from one level to another level. The conductivity increased with increasing temperature, this was a physical characteristic of semiconductors and it's corresponding to the extrinsic conductivity mechanism[24]. The changes of conductivity in this region depend on the impurity energy levels. At low temperature all the trapped electrons exist in the deep traps and with increasing temperature some of the trapped electrons could be excited to shallow traps or conduction band contributed to the conduction process. The increases of temperature did not alter the value of space-charge, but increased its fraction in the conduction band and this led to an exponential increase of σ_{dc} with the reciprocal of the absolute temperature. When CTO and CSO was sensitized with PHRBP complexes, then the DC field applied to the samples Ti/Sn atoms could be easily ionized because of generation of excess electron in parent lattices. These excess electrons increased the shallow traps below the conduction band. Due to this, there was an increase in donor concentration and hence a consequent increase in electrical conductivity for dye sensitized samples. Thus, there was a corresponding decrease in activation energy. The high temperature conductivity was a thermally activated excitation of charge carriers from grain boundaries to the region of the grains[25,26].

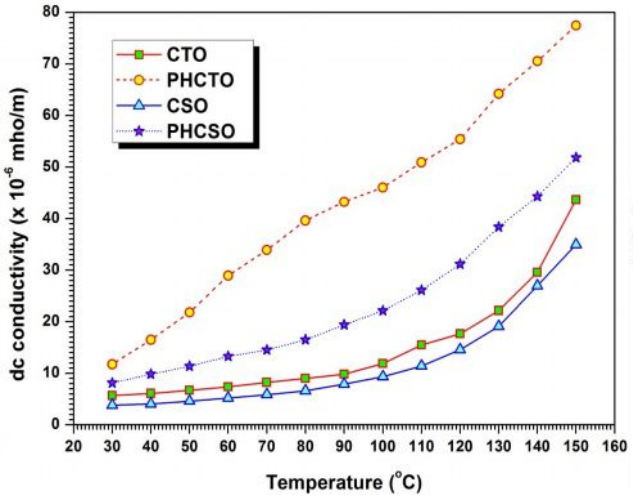

Fig 3.2.1

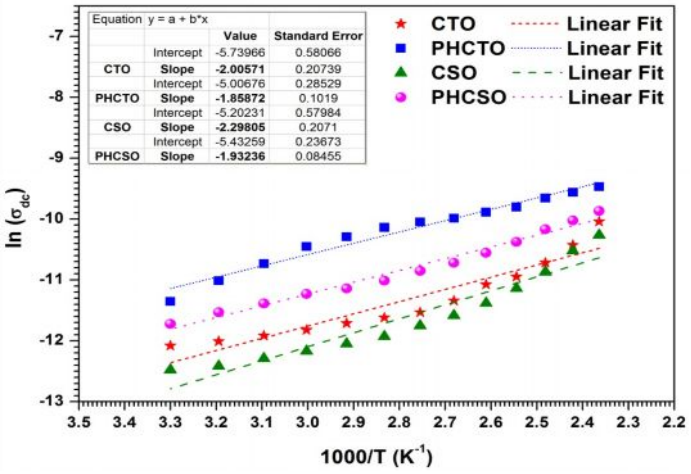

Fig 3.2.2

Fig 3.2.1 DC conductivities for desensitized and sensitized CTO and CSO nanocrystals for different temperatures

Figure 3.2.2 A plot of 1000/T *vs* Ln σ_{dc} for desensitized and sensitized CTO and CSO nanocrystals for different temperature

Table 3.2.1 DC activation energy values for desensitized and PHRBP complexes sensitized CTO and CSO nanocrystals

Sample name	**ΔE_{dc} ± 0.004 eV**	**σ_o ±0.534 Ω^{-1} m^{-1}**
CTO	0.173	-5.739
PHCTO	0.160	-5.006
CSO	0.198	-5.202
PHCSO	0.167	-5.432

Figure 3.2.3 showed the variation of dielectric constant (ε_r) with the temperature at 1 kHz for CTO, PHCTO, CSO and PHCSO samples. It was observed that the ε_r increased with increase in temperature for all the samples. The ε_r for PHRBP complexes sensitized CTO and CSO samples were lesser than that of corresponding desensitized samples at all temperatures studied in the range of 30 to 150 ºC. Figure 3.2.4 showed the variation of dielectric loss (tan δ) with the temperature at 1 kHz for CTO, PHCTO, CSO and PHCSO samples. It was observed that the tangent loss increases with increase in temperature for all the samples. The increase in tan δ of PHCTO and PHCSO (PHRBP complexes sensitized) samples was very high by 6 and 2 orders at room temperature when compared to CTO and CSO samples respectively. The rapid increment in the value of tan δ might be due to release of space charges by the dye sensitizer material[27].

The study of the temperature-dependent on AC conductivity was an important source of information about the transport phenomenon in materials. The capacitance (C) and dielectric loss factor (tanδ) measurements were carried out to an accuracy of ± 1 % with Agilant 4284A LCR meter in the temperature range of 30 - 150^{o}C and with fixed 1 kHz frequency. Figure 3.2.5 showed the variation of AC conductivity (σ_{ac}) with the temperature at 1 kHz for CTO, PHCTO, CSO and PHCSO samples. It was observed that the σ_{ac} increased with increase in temperature for all the samples also σ_{ac} for dye sensitized samples was higher than that of desensitized samples. The Figure 3.2.6 showed that the conductivity curve Ln σ_{ac} *vs* 1000/T increased linearly by increasing the temperature. This indicated that the hopping conduction was currently the dominant transport mechanism, originating from different localized states in the gap and was a thermally activated process (28). The AC activation energy (ΔE_{ac}) had been calculated for desensitized and sensitized CTO and CSO samples and was listed in Table 3.2.2. It was clear that for PHRBP complexes sensitized CTO and CSO samples, the AC activation energy was found to be lower than that of desensitized samples (CTO and CSO). Moreover, the dye sensitized samples (PHCTO and PHCSO) enhanced the electron jumps between the localized states; consequently, the activation energy ΔE_{ac} decreased when compared with desensitized samples (CTO and CSO).

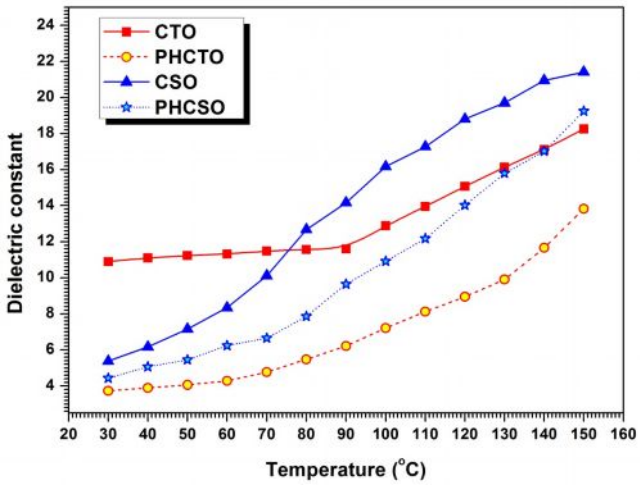

Fig 3.2.3

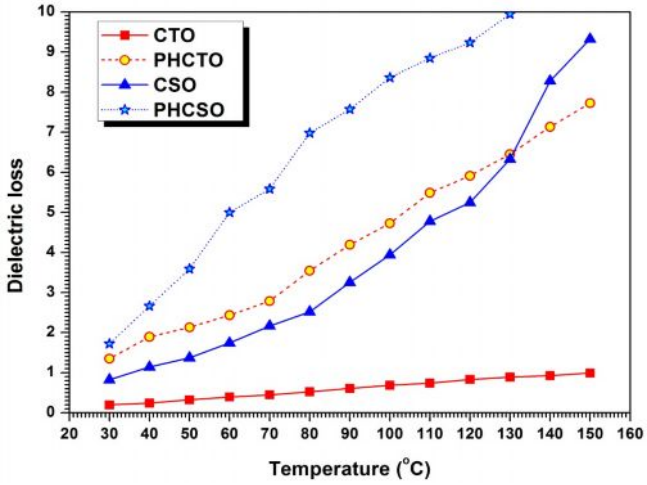

Fig 3.2.4

Fig 3.2.3 & Fig 3.2.4 The variation of dielectric constants & dielectric loss with temperature at 1 kHz frequency for desensitized and sensitized CTO and CSO nanocrystals

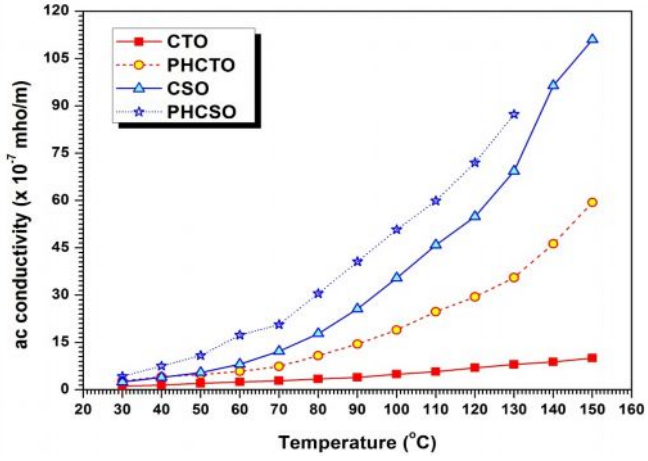

Fig 3.2.5

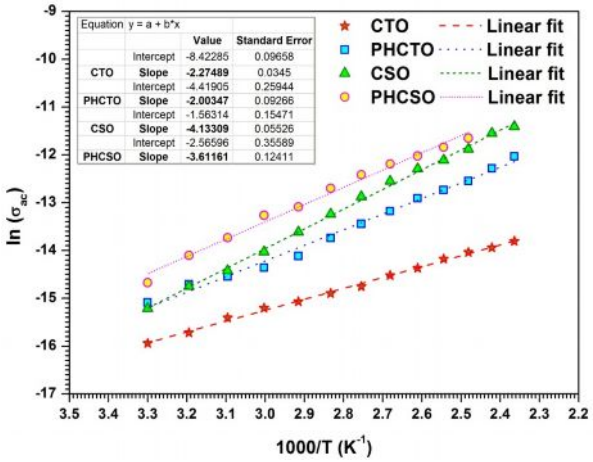

Fig 3.2.6

Fig 3.2.5 The variation of σ_{ac} with the temperature at 1 kHz frequency for desensitized and sensitized CTO and CSO nanocrystals

Fig 3.2.6 A plot of 1000/T *vs* Ln σ_{ac} for desensitized and sensitized CTO and CSO nanocrystals for different temperatures at 1 kHz frequency

Table 3.2.2 AC activation energy values for desensitized and PHRBP complexes sensitized CTO and CSO nanocrystals

Sample name	ΔE_{ac} ± 0.007 eV	σ_o ±0.216 Ω^{-1} m^{-1}
CTO	0.196	-8.421
PHCTO	0.172	-4.419
CSO	0.356	-1.563
PHCSO	0.311	-2.565

Conclusions

The photoconductivity and electrical conductivity properties of phenyl hydrazine substituted ruthenium(II) bipyridine dichloride complex (PHRBP) coated on the disc shaped pellets of Cd^{2+} doped TiO_2 (CTO) and Cd^{2+} doped SnO_2 (CSO) samples were found to be nearly 2 times larger than that of uncoated nanosamples. Recently, mesoporous TiO_2 nanoparticles showed a drastically enhanced photoelectrochemical response under visible light irradiation after entrapping a photosensitizer molecule (dye) inside the mesopores. In the present study, the dye sensitized samples (PHCTO, PHCSO) produces enhanced dark and photocurrents roughly 3 times higher than that of dye sensitized mesoporous TiO_2 nanoparticles. The efficient synthesis strategy and enhanced photoresponse of these pure and doped TiO_2 and SnO_2 semiconducting nanoparticles could make easier to design other semiconductor oxides and their applications in photon-to-electron conversion processes. Thus the present investigation concluded that Cadmium doped TiO_2, SnO_2 semiconductor oxide layer coated with phenyl hydrazine substituted ruthenium(II)bipyridine dichloride complexes act as the best materials for DSSC to get higher efficiency when compared to other materials in the present study.

References

1. O'Regan, B and Gratzel, M , A low-cost, high-efficiency solar cell based on dye sensitized colloidal TiO_2 films, Nature, 1991, 353, 737-740.
2. Arthi G , Archana J, Navaneethan M , Ponnusamy S, Hayakawa Y, .Muthamizhchelvan C, Synthesis of TiO_2 nanotubes from prepared TiO_2 nanoparticles by hydrothermal route and dye sensitized solar cell characteristics, International Journal of ChemTech Research, 2015, 7, 1563-1568.

3. Jositta Sherine, Gnaneshwar PV, Pandiyarasan Veluswamy, Synthesis and Characterization of Fabric coated with Nano Titanium oxide prepared using sol-gel, hydrothermal & Sonochemical technique, International Journal of ChemTech Research, 2015, 7, 1125-1134.
4. Firas H and Abdulrazzak, Enhance photocatalytic Activity of TiO_2 by Carbon Nanotubes , International Journal of ChemTech Research, 2016, 9, 431-443.
5. Veerathangam K, Muthu Senthil Pandian, Ramasamy P, Synthesis and characterization of cadmium sulfide (CdS) quantum dots (QDs) for quantum dot sensitized solar cell applications, International Journal of ChemTech Research, 2014, 6, 5396-5399.
6. Deepa K, Senthil S , ShriPrasad S and Madhavan J, CdS quantum dots sensitized solar cells, International Journal of ChemTech Research, 2014, 6, 1956-1958.
7. Kanne Shanker , Rondla Rohini, P, Muralidhar Reddy and Vadde Ravinder ,Tetraaza Macrocyclic, Ruthenium (II) Complexes: Synthesis, Spectral and Catalytic Studies, International Journal of ChemTech Research, 2009, 1, 300-307.
8. Sharma D M, Gangrade S D, Bakshi, J, John S, Ruthenium Complexes: - Potential candidate for Anti-Tumour Activity A.R., International Journal of ChemTech Research, 2014, 6, 828-837.
9. Pushpa Ratre and Devendra Kumar, Spectrophotometric Determination of Complexation of Ruthenium (IV) with 2-[(5-Bromo-2-Pyridylazo)]-5- Diethylaminophenol and N-Hydroxy-N, N'-Diphenyl benzamidine, International Journal of ChemTech Research, 2014, 6, 236-247.
10. Venkateswara Reddy P, Sankara Reddy B and Venkatramana Reddy S, Synthesis and Properties of Al doped SnO_2 Nanoparticles, International Journal of ChemTech Research, 2014, 6, 2168-2170.
11. Saravanakumar M, Agilan S , Muthukumarasamy N , Rukkumani V , Marusamy A , Uma mahshwari P ,Ranjitha A, Photoluminescence Studies on Nanocrystalline Pure and Cr Doped Tin Oxide Powder, International Journal of ChemTech Research, 2014, 6, 5429-5432.
12. Saravanan N , Ponnusamy S , Shri Prasad S, Joseph V, Synthesis and Characterization of SnO_2 Quantum Dots, International Journal of ChemTech Research, 2014, 6, 600-603.
13. Ratchagar V and Jagannathan K, Influence of pH on particle size and optical band gap of SnO_2 Nanomaterials, International Journal of ChemTech Research, 2015, 7, 1433-1437.
14. Blessi S, Maria Lumina Sonia, M , Vijayalakshmi ,S and Pauline, S, Preparation and characterization of SnO_2 nanoparticles by hydrothermal method, International Journal of ChemTech Research, 2014, 6, 2153-2155.
15. Saravanan N, Shri Prasad S , Ponnusamy S and Joseph V, Ultrasonic-Assisted Wet Chemical Synthesis and Characterization of Cu doped SnO_2 nanoparticles,International Journal of ChemTech Research, 2015, 7, 1574-1577.
16. Subramanyam K , Sreelekha N , Murali G , Giribabu G , Vijayalakhmi RP, Influence of Co Doping on structural and Optical properties of SnO_2 Nanoparticles , International Journal of ChemTech Research, 2014, 6, 2051-2053.
17. Chitra S**,** Easwaramoorthy D, Nalini Jayanthi S and Shanthi S, Structural and Optical properties of pure and transition metal ion doped SnO_2 Quantum Dots, International Journal of Chemtech Research, 2014,6, 4722-4728.
18. Chitra, S and Easwaramoorthy, D, Effect of divalent metal dopant on the Structural and Optical properties of TiO_2 quantum dots, International Journal of chemtech Research, 2015, 7, 1930-1937.
19. Chitra, S and Easwaramoorthy, D Studies on Ruthenium Bi-pyridine Complexes, Advanced studies in theoretical physics, 2013, 7, 1221-1229.
20. Praveen, VN and Mahadevan, CK, Electrical measurements on ZTS single crystals, Indian Journal of Physics, 2005, 79, 639-642.
21. Mahadevan, CK and Jeyakumari, K 2008, Electrical measurements on multiphased $(NaCl)_x(KCl)_{y-x}(KBr)_{1-y}$ single crystals, Physica B: Condensed Matter, 2008, 403, 3990-3996.
22. Selvarajan, G and Mahadevan, CK, Studies on $(NaCl)_x$ $(KBr)_{y-x}$ $(KI)_{1-y}$ solid solutions: 2. Electrical measurements, Journal of Materials Science, 2006, 41,8218-8225.
23. Patra, AK, Das, SK and Bhaumik, A, 'Self-assembled mesoporous TiO2 spherical nanoparticles by a new templating pathway and its enhanced photoconductivity in the presence of an organic dye', Journal of Materials Chemistry, 2011, 21, 3925.
24. Condeles, JF, Netto, TG and Mulato, M, 'Lead iodide films as X-ray sensors tested in the mammography energy region', Nuclear Instruments and Methods in Physics Research Section A: Accelerators, Spectrometers, Detectors and Associated Equipment, 2007, 577, 724-728.

25. Mahrous, S, Darwish, KA, Mounir, M and Mohsen, F, Effect of 1-chloro-2, 3-epoxy-propane on the conduction mechanism in polyvinyl chloride, Materials Letters, 1995, 23, 331-334.
26. Seoudi, R, Shabaka, AA, Kamal, M, Abdelrazek, EM and Eisa, W, Dependence of spectroscopic and electrical properties on the size of cadmium sulfide nanoparticles, Physica E, 2012, 45, 47-55.
27. Glinchuk, MD, Bykov, IP, Kornienko, SM, Laguta, VV, Slipenyuk, AM, Bilous, AG, V'yunov, OI and Yanchevskii, OZ, Infuence of impurities on the properties of rare-earth-doped barium titanate ceramics, Journal of Materials Chemistry, 2000, 10, 941-947.
28. Farid, AM and Bekheet, AE, AC conductivity and dielectric properties of Sb_2S_3 films, Vacuum, 2000, 59, 932-939.

*****